RSC Advances

ROYAL SOCIETY OF CHEMISTRY

www.rsc.org/advances

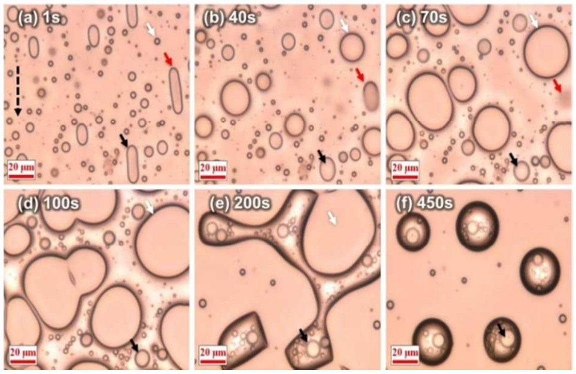

Two mechanisms in generating core-shell droplets, namely the rupture of blend films and the disintegration of compound threads, were identified.

Cite this: DOI: 10.1039/c0xx00000x

www.rsc.org/xxxxxx

Communication

Formation and Dynamics of Core-Shell Droplets in Immiscible Polymer Blends

Y. J. Huang,*[a] M. Q. Kong,[a] G. L. Chen,[a] Q. Yang,[a] and G. X. Li[a]

Received (in XXX, XXX) Xth XXXXXXXXX 20XX, Accepted Xth XXXXXXXXX 20XX
DOI: 10.1039/b000000x

Two possible mechanisms in generating core-shell droplets, namely the rupture of blend films and the disintegration of compound threads, were identified in immiscible polymer blends with high viscosity. The deformation and relaxation behavior of core-shell droplets was shown to be intimately related to the core-to-shell diameter ratio (R_{cs}).

Core-shell morphology, also referred to as double emulsion or encapsulated structure, is a particular structure characteristic of a dispersed phase containing another immiscible phase in a matrix. Core-shell droplets are promising in various functional applications such as drug transporting and releasing, and their functionalities are closely related to their microstructure and dynamics during processing and application.[1] The accurate generation and manipulation of core-shell structure in low molecular weight liquids could be achieved by utilization of microfluidic techniques.[2-4] However, a comprehensive knowledge about the dynamics of core-shell structure (such as formation, deformation and relaxation) especially under flow is still scarce, which greatly limits the exploiting of their potentials in various applications. Available studies are mainly limited to numerical simulations. For instance, Kan *et al*.[5] explored the dynamics of the core-shell structure by a leukocyte model with the Eulerian–Lagrangian algorithm. They found that if the time scale of the core was comparable to that of the shell, the compound droplet would behave like a homogeneous and simple droplet. But disparate time scales between the core and the shell resulted in a rapid initial recoil of the droplet, followed by a slower relaxation during which the core and shell interacted with each other. By using a level set representation of the interface, Smith *et al*.[6] constructed a phase diagram to describe the flow-induced morphologies over a range of capillary numbers (Ca) and interfacial tension ratios (κ) of the core to outer droplet. In the case of small κ and low Ca, the core-shell droplet would break into a series of encapsulated daughter droplets; at large κ the core would undergo a little deformation then formed a bulge which caused the outer droplet ends to pinch off. In case of small κ and high Ca, the droplet would relax back into a sphere. Despite of fruitful results obtained numerically, direct experimental evidence about the structure formation and stability of core-shell droplets is still lacking possibly due to the fast dynamics of low-viscosity liquids.

Fortunately, core-shell morphology can also be obtained in binary or ternary immiscible polymer blends during melt mixing[7-13] or in partial miscible blends via viscoelastic phase separation.[14,15] In consideration of their slow structure dynamics and distinct phase boundary, immiscible polymer blend melts with high viscosity may serve as ideal model systems for the study of the dynamics of core-shell droplets under flow. Thermodynamically, the formation of core-shell droplets in ternary blends (especially copolymer-compatibilized blends[16]) is determined by several parameters such as the component ratio and interfacial tension between components, and can be predicted using the spreading coefficient or a minimal surface free energy model.[7-9] The elasticity is found to act as an additional interfacial tension under shear conditions which will influence the encapsulation behavior of phases.[8-10] The formation of core-shell morphology in binary polymer blends usually requires a change in the feeding sequence or other operating parameters, in which phase inversion or uneven mixing is usually involved.[11-13] For example, Favis *et al.*[11] found that for polypropylene (PP)/polycarbonate (PC) blends with a volume fraction of 75/25, core-shell structure, in which PC was the dispersed phase with spherical PP sub-inclusions, was obtained in the PP matrix by adjusting the mixing time in an impeded phase inversion. However, the detail formation mechanism and structure dynamics of these core-shell droplets have not, so far, been touched.

Here, we report an *in-situ* experimental investigation about the formation and evolution dynamics process of core-shell droplets in an immiscible polystyrene (PS)/high-density polyethylene (HDPE) blend prepared via a two-step mixing strategy. Commercial polystyrene (PS) and high-density polyethylene (HDPE) with a melt flow index (MFI) of 7.0 g/10 min (5 kg, 200°C) and 7.6 g/10 min (10 kg, 220°C) were provided by Taihua Plastic (Ningbo) Co., Ltd and Dushanzi Petrochemical Co. (China), respectively. The zero-shear viscosities of HDPE and PS at 200°C were 1020 Pa·s and 5030 Pa·s, respectively. The interfacial tension σ between PS and HDPE was 5.2 $mN{\cdot}m^{-1}$ according to the deformed drop retraction method (DDRM).[17] A blend with weight ratio of HDPE:PS=80:20 was prepared using a Haake Rheomix 600 mixer operating at 200°C and 50 rpm for 3 min with the addition of 0.3 wt.% antioxidant 1010. A shear-optical system, which combined a microscope (Olympus BX51, Japan) and a double-side heated Cambridge shearing stage (CSS-450, Linkam Scientific, UK) was utilized to study the deformation and relaxation of core-shell structure *in-situ* under well-controlled shear conditions (please refer to Ref [18-20] for details). Typically, a PS/HDPE blend film (~100 µm in thickness) was sandwiched between two PS disks (1 mm in thickness) and melted at 200°C in the shearing stage (see Scheme 1 for the sample configuration). The sandwiched sample was then sheared at 0.5 s^{-1} at a gap space of 1500 μm for 600 s to produce core(PS)-shell(HDPE) droplets.

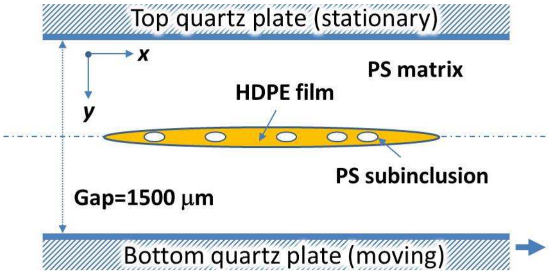

Scheme 1 Illustration of the side view of the sandwiched sample configuration for optical-shear experiments. The *x* and *y* denote the flow and rate gradient direction, respectively.

Formation of core-shell droplets. Complicated morphologies including dispersed droplets, compound threads and films were produced in the sandwiched PS/HDPE blend sample during/after shearing. Two mechanisms in generating core-shell droplets were identified. The first mechanism for the produce of core-shell droplets is the spontaneous rupture of thin blend film containing subinclusions during relaxation. Figure 1 displays the rupture process of a PS/HDPE blend film containing PS subinclusions with diameter of 1~10 μm in the PS melt after shearing at 200°C and 0.5 s^{-1} for 600 s. The film thickness was estimated to be about 10 μm based on the volume conservation of these compound droplets produced in Figure 1f, which was comparable to the largest size of PS subinclusions. The rupture of blend film started from the growth of holes (Figure 1a), which was related to the spontaneous rupture of thin films in the presence of small thickness fluctuations under the driving of interfacial tension.[21] A transient network structure was then formed due to the continuous expansion of these holes (Figure 1d-e). Then core-shell droplets with various diameters and numbers of subinclusion droplets were produced due to the disintegration of this transient network. During the gradual rupture of network structure, the coalescence of PS subinclusion droplets and the merging of subinclusion droplets into the PS matrix were also found.

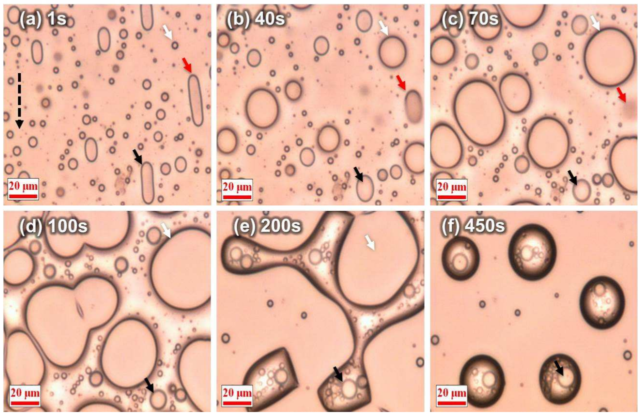

Figure 1 Formation process of core-shell droplets via the rupture of PS/HDPE blend thin film in PS matrix during annealing after sheared at 0.5 s^{-1} and 200°C for 600 s. The dash arrow denotes the flow direction. PS droplet which would constitute the core was denoted by black arrow. The hole from which the film ruptures is marked with the white arrow. The PS subinclusion droplet which will merge into the matrix is marked with the red arrow. The scale bars denote 20 μm.

The second mechanism in generating core-shell droplets was the disintegration of PS/HDPE compound threads via Rayleigh instability. As shown in Figure 2, for PS/HDPE films undergoing continuous shear flow at 0.5 s^{-1}, some slender compound threads were formed in the flow direction after the rupture of films. These compound threads consisted of elongated PS cores embedded in the HDPE shells. These slender compound threads were unstable under shear flow or during quiescent melt annealing. The development of Rayleigh instability was observed both for the HDPE shell and PS core of compound threads, which also led to the formation of near-spherical core-shell droplets in the PS matrix. Some fragments of slender compound droplets with small aspect ratio retracted into ellipsoidal droplets which containing several large PS cores. Coalescence of large PS cores was observed in the late stage of relaxation of compound droplets. Most of core-shell droplets generated via this mechanism contained only one PS core therein. Above results suggest that the two-step melt mixing method represents a simple and efficient process in preparing core-shell droplets in viscous polymer blends.

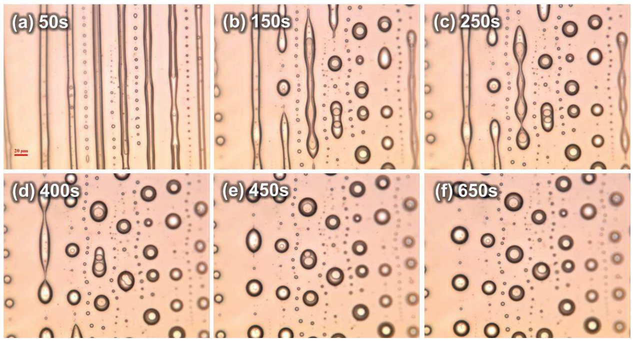

Figure 2 Formation process of core-shell droplets via the relaxation of PS/HDPE compound threads in PS matrix after continuously shearing at 0.5 s^{-1} for 2000 s. The scale bar denotes 20 μm.

Deformation of core-shell droplets under shear. The deformation of core-shell droplets was realized by applied various shear strains (γ=0~4) to the droplets obtained. The shear strains were set within 4 to ensure that core-shell droplets after shearing could relax to their equilibrium state. The deformation behavior of a series of core-shell droplets with core-to-shell diameter ratio (R_{cs}) ranged from 0.25 to 0.56 was considered. Figure 3 displayed the shape evolution of a core-shell droplet with core diameter about 30 μm and shell diameter about 56 μm (namely R_{cs}=0.54) at a shear rate of 0.5 s^{-1}. With increasing shear strain (up to γ=3), the shell evolved gradually into a spindle shape (Figure 3a~d). The droplet was stretched in the shearing direction while it kept almost a constant width in the direction perpendicular to the shear flow, suggesting that the droplet became flat in the shear gradient direction during deformation. When the shear strain further increased to γ=4, as shown in Figure 3(e), the core-shell droplet became narrower in the width and attained a very interesting shape. According to the relative brightness of two tips of the shell, the side view of this highly deformed core-shell droplet was sketched out in Figure 3(f). It was showed that the deformation of droplet was asymmetric. The droplet formed two tips near the bottom shear plate and top shear plate of shear cell, respectively. The shape was significant different from the flat ellipsoid shape of pure droplet reported[22] and the slender shape predicted[6] under large shear strains. The formation of this asymmetric shape may be the comprehensive result of the presence of a less deformable core in the droplet and the drag force[23] of the PS matrix melt acted on the outer HDPE shell in the flow direction. When the shear strain exceeded 7.5, this core-shell droplet would break up into pure HDPE droplets with diameter about 10~15 μm dispersed in the PS matrix. There existed a critical R_{cs} about 0.35 for the deformation behavior of cores. When R_{cs} was larger than the critical value, the core elongated apparently under shear. When R_{cs} was smaller than the critical value, the core could hardly be deformed.

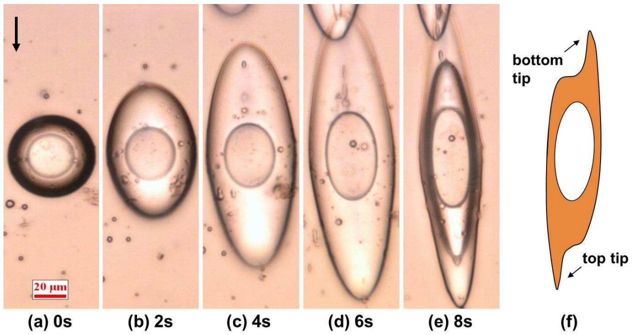

Figure 3 (a)-(e): The deformation of a core-shell droplet with a core-to-shell diameter ratio of 0.54 after shearing at 0.5 s^{-1} for different times. (f): the schematic drawing of the side view of deformed droplet in (e). The scale bar denotes 20 μm.

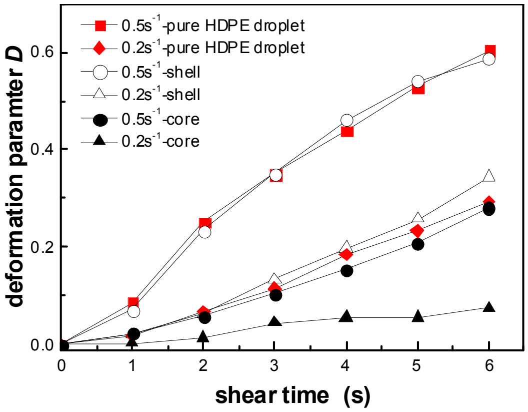

Figure 4 Deformation parameters of the core-shell droplet shown in Figure 3 as a function of shear time. The deformation data of a pure HDPE droplet with a same diameter (~56 μm) to that of core-shell droplet are also presented for comparison.

Figure 4 compares the deformation parameters for the core and shell of droplet shown in Figure 3 subjected to different shear strains at 0.2 s^{-1} and 0.5 s^{-1}. The deformation parameter is defined as $D=(L-W)/(L+W)$, where L and W is the droplet length parallel to and vertical to the shear direction, respectively. The deformation parameter of core and shell both increased almost linearly with the shear time. However, the deformation behavior of shell was almost identical with that of pure HDPE droplet with a same diameter. And the deformation parameter of core was always smaller than that of shell regardless of the shear rate or shear strain applied. The rigidity against deformation displayed by the core could be ascribed to the higher viscosity (5030 Pa·s) and smaller size of core compared with that of the shell (1020 Pa·s). The overshoot in the core length under shear flow as predicted theoretically for a Newtonian droplet both in Newtonian fluid[6] and non-Newtonian fluids[24] was observed here. The reason may be ascribed to the large R_{cs} of the core-shell droplet or the viscoelastic nature of both droplet phase and matrix phase in the present HDPE/PS blend.

Relaxation of core-shell droplets after deformation. After the cessation of shear flow, the deformed core-shell droplet would retract into its equilibrium shape under the driving of the interfacial tension between components. Figure 5 shows the relaxation process of a core-shell droplet with R_{cs}=0.52 after shearing at 0.5s^{-1} for 4 s. As shown in Figure 5, the HDPE shell relaxed into a sphere gradually in ~450 s with an initial small narrowing in the shell width. However, the PS core displayed an interesting relaxation behavior. The core retracted into a sphere quickly in the initial relaxation stage (0~90 s) and then it was over-squeezed by the retracting outer HDPE shell in the long axis direction of shell into an ellipsoid in the intermediate stage (90 s~160 s). This over-squeezed PS core then relaxed gradually into a spherical shape during the retraction process of the outer HDPE shell. It should be noted that the lensing effect should be marginal here since the refraction indices of PS (n=1.58) and HDPE (n=1.51) are close and should not lead to nonspherical shape of subinclusions.

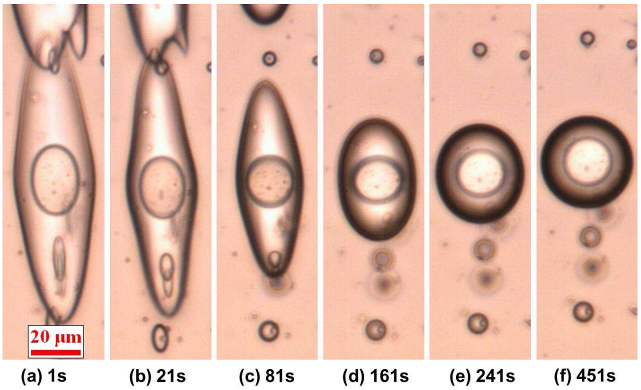

Figure 5 Relaxation process of a core-shell droplet (R_{cs}=0.52) after shearing at 0.5 s^{-1} for 4 s. The scale bar denotes 20 μm.

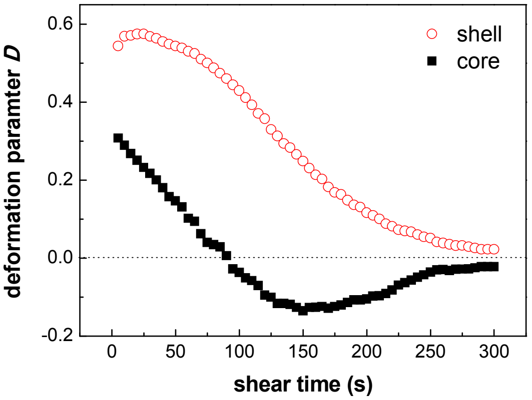

Figure 6 Deformation parameter (D) of the core and that of the shell as a function of the relaxation time after shearing at 0.5 s^{-1} for 4 s. The data is obtained from Figure 5.

Figure 6 shows that temporal evolution of D for the shell and core during shape relaxation. It was clear that the D of core declined to zero and the core recovered a spherical shape at 90 s, which was more rapid than that of the outer shell. The *D* of PS core declined continuously to -0.135 since then, implying the core was over-squeezed. After that, the negative *D* of inner core and the positive *D* of outer shell changed slowly to zero.

This particular over-squeezing phenomenon observed during the relaxation of core-shell droplets has been predicted by theory and simulation.[5, 25, 26] It was proposed that the over-squeezing of core should originate from the non-synchronization or mismatch between the relaxation dynamics of core and that of the shell. It can be understood simply as a minimization of total interfacial energy. When the *D* of core approaches zero during its fast relaxation process, the outer interface has not yet regained its equilibrium shape due to its relatively larger size. The internal flow field caused by the retracting outer interface will deform the core to minimize the total interfacial energy. Here, this over-squeezing phenomenon is observed experimentally in polymer melts with high viscosities and is found to be closely correlated with the R_{cs} of core-shell droplets.

Figure 7 further reveals the dependence of normalized *D* (D/D_0) as a function of relaxation time for a series of core-shell droplets with different R_{cs} values. For core-shell droplets with R_{cs}<0.35, the cores relaxed to a sphere rapidly and kept a near-spherical shape during the relaxation of outer shell. As a result, the core appeared to be less deformable than the core when it was sheared. While, for core-shell droplets with R_{cs}>0.35, the cores all undergone the over-squeezing process during shape relaxation. Although core-shell droplets with R_{cs} value close to unity were not found during experiments, it is reasonable to speculate that the inner PS cores of these droplets should display almost identical relaxation dynamics to that of outer HDPE shells due to their severe geometry limitation. In a word, the over-squeezed core could be observed for core-shell droplets only with a moderate R_{cs} value.

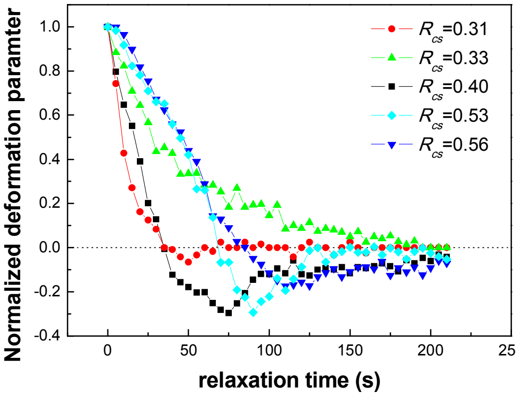

Figure 7 Normalized *D* of core vs relaxation time for core-shell droplets with different R_{cs} after shearing at 0.5 s^{-1} for 4 s.

Conclusions

In-situ optical-shear experiments indicated that the two-step melt mixing method was efficient in producing core-shell droplets in the high viscous PS/HDPE blends. There were two possible mechanisms for the formation of core-shell droplets, namely the breakup of blend film and the disintegration of compound thread. The deformation of core-shell droplets under shear strains was similar to that of pure HDPE droplets of equal size. The core-to-shell diameter ratio (R_{cs}) played an important role in governing the deformation and relaxation dynamics of the core. For the present system, the core displayed rigidity resisting deformation and relaxation when R_{cs} was smaller than a critical value of 0.35. When R_{cs} was larger than this critical value, the non-synchronization between the core and the shell would cause the core to be over-squeezed in the long axis direction of shell during the relaxation process. These findings provide some direct experimental evidences for available numerical results about the dynamics of core-shell droplets. However, to provide necessary knowledge about the delicate manipulation of core-shell droplets in various functional applications, more systematic works on the role of component viscoelasticity and core-shell structure parameters are required.

Acknowledgments

We are grateful to the financial support from the National Natural Science Foundation of China (51373109, 51121001), the Fundamental Research Funds for the Central Universities (2013SCU04A02), and the Innovation Team Program of Science & Technology Department of Sichuan Province (Grant 2013TD0013).

Notes and References

[a] *College of Polymer Science and Engineering, State Key Laboratory of Polymer Materials Engineering, Sichuan University, Chengdu,610065, China*
Corresponding Authors
**E-mail: hyj@scu.edu.cn (Y.H.).*
**E-mail:guangxianli@scu.edu.cn (G.L.)*

1 C. Miesch, I. Kosif, E. Lee, J. K. Kim, T. P. Russell, R. C. Hayward and T. Emrick, *Angew. Chem. Int. Edit.*, 2012, **51**, 145-149.
2 W. Wang, R. Xie, X.-J. Ju, T. Luo, L. Liu, D. A. Weitz and L.-Y. Chu, *Lab Chip*, 2011, **11**, 1587-1592.
3 J.-H. Xu, X.-H. Ge, R. Chen and G.-S. Luo, *RSC Advances*, 2014, **4**, 1900-1906.
4 A. Schmit, L. Courbin, M. Marquis, D. Renard and P. Panizza, *RSC Advances*, 2014, **4**, 28504-28510.
5 H.-C. Kan, H. S. Udaykumar, W. Shyy and R. Tran-Son-Tay, *Phys. Fluids*, 1998, **10**, 760-774.
6 K. A. Smith, J. M. Ottino and M. O. de la Cruz, *Phys. Rev. Lett.*, 2004, **93**, 204501.
7 H. F. Guo, S. Packirisamy, N. V. Gvozdic and D. J. Meier, *Polymer*, 1997, **38**, 785-794.
8 T. S. Valera, A. T. Morita and N. R. Demarquette, *Macromolecules*, 2006, **39**, 2663-2675.
9 J. Reignier, B. D. Favis and M. C. Heuzey, *Polymer*, 2003, **44**, 49-59.
10 T. S. Omonov, C. Harrats and G. Groeninckx, *Polymer*, 2005, **46**, 12322-12336.
11 B. D. Favis, C. Lavallee and A. Derdouri, *J. Mater. Sci.*, 1992, **27**, 4211-4218.
12 Q. Li, Y. J. Huang, S. T. Xi, Q. Yang and G. X. Li, *AIChE J.*, 2013, **59**, 4373-4382.
13 J. D. Martin and S. S. Velankar, *AIChE J.*, 2008, **54**, 791-801.
14 J. Jose, K. Joseph, J. r. Pionteck and S. Thomas, *J. Phys. Chem. B*, 2008, **112**, 14793-14803.

15 P. Jyotishkumar, P. Moldenaers, S. M. George and S. Thomas, *Soft Matter*, 2012, **8**, 7452-7462.

16 R. Fayt, R. Jerome and P. Teyssie, *Journal of Polymer Science Part C: Polymer Letters*, 1986, **24**, 25-28.

17 A. Luciani, M. F. Champagne and L. A. Utracki, *J. Polym. Sci. Pol. Phys.*, 1997, **35**, 1393-1403.

18 M. Q. Kong, Y. J. Huang, G. L. Chen, Q. Yang and G. X. Li, *Polymer*, 2011, **52**, 5231-5236.

19 Y. Mei, Y. J. Huang, Q. Yang and G. X. Li, *Polymer*, 2012, **53**, 5413-5422.

20 M. Q. Kong, Y. J. Huang, Y. D. Lv, Q. Yang and G. X. Li, *Polymer*, 2014, **55**, 4348-4357.

21 W. W. Zhang and J. R. Lister, *Phys. Fluids*, 1999, **11**, 2454-2462.

22 R. Hayashi, M. Takahashi, H. Yamane, H. Jinnai and H. Watanabe, *Polymer*, 2001, **42**, 757-764.

23 D. J. Chen, R. Cardinaels and P. Moldenaers, *Langmuir*, 2009, **25**, 12885-12893.

24 P. Yue, J. J. Feng, C. Liu and J. Shen, *Phys. Fluids*, 2005, **17**, 123101.

25 H. A. Stone and L. G. Leal, *J. Fluid. Mech.*, 1990, **211**, 123-156.

26 K. A. Landman, *AIChE J.*, 1985, **31**, 567-573.